
Article:
Wang, Y., Shi, X., Zhao, X. et al. (2026) Diabetes impairs post-stroke angiogenesis and BBB integrity accompanied by dysregulated Slit2/Robo-CRTC1 pathway. Cellular and Molecular Neurobiology. ISSN: 0272-4340

https://doi.org/10.1007/s10571-026-01811-w

ORIGINAL RESEARCH | Article in Press

Diabetes Impairs Post-stroke Angiogenesis and BBB Integrity Accompanied by Dysregulated Slit2/Robo-CRTC1 Pathway

Yanping Wang · Xuemei Shi · Xiaoyun Zhao · Xudong Lu · Jingxia Gu · Hui Guo · Yihui Wang · Xiaoqiang Wu · Congying Xu · Minghui Shen · Yufei Shen · Chun Guo · Yanan Hao · Shuxia Qian · Xinchun Jin

Received: 16 March 2026 / Accepted: 17 August 2026

Abstract

Diabetes Mellitus (DM) is a major comorbidity that exacerbates ischemic brain injury and hinders functional recovery following stroke. Given that angiogenesis and the maintenance of blood-brain barrier (BBB) integrity are essential for neurorestoration, understanding how DM influences these processes and the molecular mechanisms involved is critical for improving clinical outcomes. To investigate these effects, a type 1 DM model was established in six-week-old mice via intraperitoneal injections of streptozotocin (60 mg/kg/day for 5 days), with success confirmed by blood glucose testing two weeks later. Focal ischemic stroke was subsequently induced using a photothrombosis model. Functional recovery was assessed using neurological scoring, the Rotarod test, and the foot-fault test. Post-stroke neovascularization was quantified via lectin injection, while BBB integrity was evaluated through IgG leakage, pericyte coverage, and the expression of tight junction proteins (Zo-1, occludin, and claudin-5). Additionally, protein expression within the Slit2/Robo/CRTC1 pathway was analyzed 1, 7, and 14 days post-stroke using immunofluorescence and western blotting. Our results demonstrated that DM significantly impaired sensorimotor recovery and hindered reparative neovascularization in the peri-infarct area. Furthermore, DM exacerbated BBB disruption, as evidenced by increased IgG leakage, reduced expression of occludin and claudin-5, and diminished pericyte coverage. Mechanistically, DM led to a decrease in Robo1 and an increase in Robo4 expression without altering Slit2 levels. Additionally, DM further suppressed the expression of the co-transcription factor CRTC1 following the ischemic event. Our findings indicate that DM impairs post-stroke angiogenesis and BBB repair accompanied by the dysregulation of the Slit2/Robo/CRTC1 signalling pathway. These results highlight a potential therapeutic target for enhancing stroke recovery in diabetic populations.

Keywords Diabetes mellitus · Photothrombosis · Angiogenesis · BBB · Slit2/Robo · Neurological function

Yanping Wang and Xuemei Shi contributed equally to this work.

https://doi.org/10.1007/s10571-026-01811-w

Published online: 02 September 2026

Abbreviations

AIS	Acute ischemic stroke
BBB	Blood-brain barrier
DM	Diabetes mellitus
EB	Evan's blue
EC	Endothelial cells
HT	Hemorrhage transformation
I	Ischemic hemisphere
IgG	Immunoglobulin G
I/R	Ischemia/reperfusion
MCAO	Middle cerebral artery occlusion
NI	Non-ischemic hemisphere
TJPs	Tight junction proteins

Introduction

DM is a critical comorbidity that significantly increases the risk of stroke, the leading cause of global disability, while exacerbating ischemic brain injury and worsening functional outcome (Kuwashiro et al. 2013). Clinical evidence indicates that the prognosis and survival of stroke patients are positively correlated with the density of neovascularization within the ischemic hemisphere of the brain (Krupinski et al. 1994). However, post-stroke angiogenesis is a "double-edged sword": immature new vessels can increase BBB permeability (Yang and Torbey 2020). This loss of BBB integrity is the primary pathological driver of vasogenic cerebral edema and hemorrhagic transformation after stroke (Chen et al. 2022; Wang et al. 2023c). DM is known to inhibit endothelial progenitor cell-mediated angiogenesis (Peng et al. 2023), a deficit closely linked to impaired sensorimotor and cognitive recovery (Abdelsaid et al. 2015; Prakash et al. 2013). Moreover, diabetic patients face a higher risk of symptomatic hemorrhagic transformation following acute thrombolysis (Martini and Kent 2007; McCormick et al. 2008), as DM further compromises BBB integrity after stroke (Wicha et al. 2021). Despite these observations, the precise mechanisms by which DM impairs poststroke angiogenesis and BBB stabilization during the recovery phase remain poorly understood. Recent studies suggest that axon guidance factors (AGF), originally identified in the nervous system, play a pivotal role in vascular development (Adams and Eichmann 2010; Rust et al. 2019b). For example, Slit2, a secreted glycoprotein, regulates endothelial cell migration, budding, and tube formation through its Robo receptors (Coll et al. 2022; Romano et al. 2018). Specifically, the Slit2-Robo1 pathway promotes (Rama et al. 2015), whereas Robo4 inhibits (Suchting et al. 2005) pro-angiogenic activity; recombinant Slit2 reduced surgical brain injury -induced BBB hyperpermeability by modulating tight junctions (Sherchan et al. 2017). While Slit2 is known to regulate tumor angiogenesis (Beck and Plate 2009) and angiogenesis following myocardial infarction (Wong et al. 2026), its role, along with its receptors Robo1/4, in the diabetic post-stroke environment has not been established.

Furthermore, the transcriptional co-activator CRTC1 has emerged as a key regulator of the neurovascular unit. CRTC1 deficiency exacerbates BBB breakdown and hinders mouse forelimb recovery after ischemia (Yan et al. 2021). Conversely, CRTC1 expression typically decreases following MCAO, coinciding with neuronal loss (Chen et al. 2022), while its upregulation by inhibiting reactive astrocytes has been shown to improve cognition after ischemic stroke (Zhang et al. 2019). In the present study, we utilized a photothrombosis model to investigate how DM impairs post-stroke angiogenesis and BBB integrity. We specifically examined the involvement of the Slit2/Robo/CRTC1 signaling axis in these pathophysiological processes to identify potential therapeutic targets for diabetic stroke recovery.

Materials and Methods

Animal

Male C57BL/6 mice (8 weeks old), weighing 22–26 g, were provided by the Laboratory Animal Center of Capital Medical University. All animal experiments were approved by the IACUC of Capital Medical University and were performed in accordance with the NIH Laboratory Animal Care and Use Guidelines. Animals were randomly assigned to groups by the study director, who was blinded to all biometric data. Investigators were blinded to group allocation when performing all data collection. No animals were excluded for failure to achieve the predicted phenotypes.

Model

Type 1 Diabetes Mellitus Model Induction and Confirmation

Inject 1% STZ solution according to the dose of 60 mg/kg, and administer it for 5 days in a row. Once the blood glucose level reached above 13.9 mM (250 mg/dl) (Shi et al. 2018), weekly measurements continued for 4 weeks until experiments were completed (Fig. 1a).

Photothrombosis Ischemia Model

Focal ischemic stroke was induced by photothrombosis in mice, as described (Chen et al., 2024). In brief, mice were anesthetized with sodium pentobarbital (45 mg/kg, i.p) and placed in a stereotaxic apparatus (RWD, China), with the body temperature kept constant at 37.5 ± 0.5 °C by a heating pad. Rose Bengal (100 mg/kg, Sigma) was intraperitoneally injected. Five minutes later, a cold light source (diameter 2.0 mm; 24,000 lx, RWD, China) was positioned 1.5 mm lateral to the bregma of the skull, and the brain was illuminated for 20 min to initiate photothrombosis, resulting in the ischemic injury of the right motor and somatosensory cortices. The control mice underwent the same procedure without illumination. After completion of the surgical procedures, the incision was sutured, and the mice were placed in a controlled temperature condition (24–25 °C) to recover from anesthesia.

Tomato Lectin Injection to Label Functional Blood Vessels

Tomato lectin is widely used to label functional blood vessels. On the first, 7th, or 14th days after brain ischemia, it is injected through the femoral vein at a dose of 1.25 mg/kg. After 5 min of body circulation, the mice are deeply anesthetized and perfused with cold PBS and PFA. All blood vessels with blood flow will be labeled with tomato lectin. Take out the brain tissue and soak it in PFA for 4 h, followed by a 10% sucrose solution for 12 h. The embedded brain tissue is cut into 20 μm-thick frozen slices. It can be observed directly under the fluorescent microscope. The length of the functional blood vessels is analyzed statistically through the "Analyze Skeleton" function of the ImageJ software (Qi et al. 2016).

Behavior Test

Neurological Scores

The mNSS assessment consists of motor, reflex, and balance tests and can dynamically evaluate the neurological deficits at 1, 3, 7, and 14 days after reperfusion. The mNSS scores range from 0 to 7 points, and the higher the score, the more severe the neurological impairment (Du et al. 2026a).

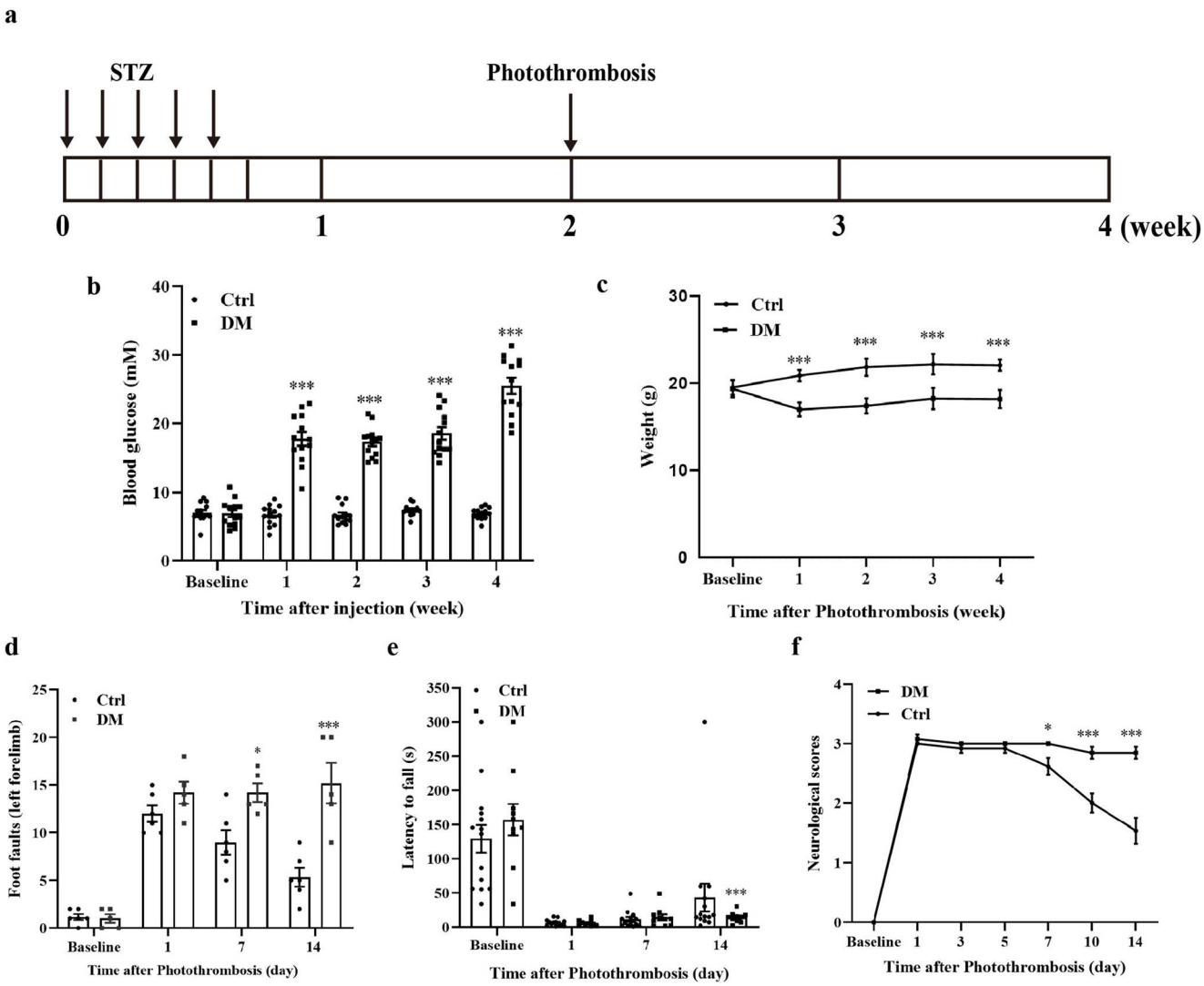

Fig. 1 DM impairs neural functional recovery after photothrombosis. **a** Experimental procedure to set up type 1 DM and photothrombosis (PT) model. STZ was injected i.p. continuously for 5 days at a dose of 60 mg/kg/day. Photothrombosis was performed after 2 weeks of STZ injection, and the brains were removed for further analysis 14 days after ischemia. The neural function was assessed. **b** Blood glucose increased significantly after a week of STZ injection, and **c** the body weight of DM mice significantly decreased compared with the Ctrl mice ($n=13$/group). **d** DM impairs motor function in the foot fault test 7 days after ischemia ($n=5$–6/group). **e** DM impairs motor function in the Rotarod test 14 days after ischemia. **f** The DM group showed significantly higher neurological scores from 7 days until 14 days compared to the Ctrl group ($n=13$/group, $^{*}P<0.05$, $^{***}P<0.001$ vs. Ctrl. Ctrl, control; DM, diabetes mellitus

Rota Rod

The rotarod test was performed to assess post-stroke motor deficits as previously described (Guo et al. 2025). A baseline level was recorded before surgery, and then detected at 1, 7, and 14 days after cerebral ischemia. Mice were placed on a 3.0-cm-diameter rotarod (Zhongshi Technology, China) and trained to stay on the rotating rod for 300 s at a rate of 5 to 40 revolutions per minute.

Foot Fault

Foot fault was tested as we previously described (Du et al. 2026c). A baseline level was recorded before surgery, and then detected at 1, 7, and 14 days after cerebral ischemia. The mice were placed on a steel gridded floor grid (35 × 25 × 25 cm) and video recorded; the grid size is about 1.2 cm^2. The number of errors (mice misplacing their forelimbs and falling off the grid) was recorded out of a total of 100 steps of the forelimbs of the mice.

BBB Leakage Detection

IgG Leakage Detection

BBB integrity could be determined by detecting IgG leakage, as we described previously (Hu et al. 2024). Briefly, the brain sections (20-μm thick) were fixed with 4% paraformaldehyde (PFA) for 20 min at room temperature, then incubated with 488-conjugated Affinity Pure Goat anti-mouse IgG (1:200, KPL) for 2 h at room temperature.

Immunofluorescence

Immunostaining was performed on C57BL/6J mice brain sections (Wang et al. 2023a). Mice were deeply anesthetized and transcardially perfused with PBS followed by 4% (wt/vol) paraformaldehyde (PFA) in PBS. Brains were harvested and fixed with 4% PFA for 4 h at 4 °C, and immersed in 30% (wt/vol) sucrose in PBS; frozen serial coronal brain sections (20 μm thick) were prepared on a cryostat (CM1900; Leica). The sections were blocked with 5% (wt/vol) BSA (Solarbio, Beijing, China) in 0.3% Triton X-100 for 2 h at room temperature. The primary antibodies are used as follows: mouse Robo1 (1: 50, Santa Cruz), mouse Robo4 (1:50, SantaCruz), rabbit Slit2 (1:200, Abcam), rabbit CD31 (1:100, Abcam), mouse CD31 (1:100, Abcam), ki67 (1:400, Abcam), rabbit PDGFR-β (1:200, Abcam, CA), mouse claudin-5 (1:200, Invitrogen). After rinsing thrice with PBS, the samples were incubated with corresponding secondary antibodies for 60 min at RT. The nucleus was stained with 4, 6-diamidino-2-phenylindole (DAPI, 1:1000, Life Technologies, Mulgrave, VIC, AUS).

Western Blot

Western blot analysis was performed as previously described (Wang et al. 2020). Tissue samples and cells were extracted using RIPA buffer (Beyotime Biotechnology, Shanghai, China) that contained protease inhibitor cocktails (Sigma, California, USA) and phosphatase inhibitor cocktail tablets (Roche Diagnostics, Basel, Switzerland) for 30 min. Protein concentrations were determined using the BCA protein assay kit (Beyotime Biotechnology, Shanghai, China). Proteins (30 μg of total protein) were loaded on 10–12% SDS-PAGE gels, and proteins were transferred to PVDF membrane (Millipore, Billerica, MA, USA) and blocked for 2 h in 5% nonfat milk in TBS-T (Tris-buffered saline and 0.1% Tween-20) for 1 h at room temperature. Membranes were then incubated with primary antibodies overnight at 4 °C. The primary antibodies used in this study included mouse Robo1 (1:500, Santa Cruz), mouse Robo4 (1:500, SantaCruz), rabbit Slit2 (1:3000, Abcam), CRTC1 (1:1000, CST), rabbit occludin, claudin-5 (1:500, Invitrogen), and GAPDH (1:5000, Boster). After incubation with primary antibodies, membranes were incubated with HRP-conjugated anti-Rabbit IgG (1:5000, Boster) and HRP-conjugated anti-Mouse IgG (1:5000, Boster) for 1 h at room temperature. The protein bands were developed with an enhanced luminescence reagent (Millipore, California, USA) and photographed with a Chemiluminescence imaging system (5200, Tanon, China).

Statistics

The data are expressed as the mean±standard error of the mean (SEM). Two-way analysis of variance (ANOVA) with repeated measures was used for behavior results. One-way ANOVA was applied to detect the difference between two groups on the same day. One-way or two-way ANOVA was used to assess the other results. The threshold for statistical significance was set at $P<0.05$. GraphPad Prism 10.6.0 (GraphPad Software, USA) was used for figure preparation, and SPSS Statistics 25 was used for statistical analysis.

Results

Diabetic Mice Exhibit Impaired Sensorimotor Recovery Following Photothrombosis

To establish the DM model, mice received daily STZ injections with a dose of 60 mg/kg for five consecutive days following a 12-hour fast (Fig. 1a). One week post-injection, mice exhibited rising blood glucose levels (Fig. 1b) and concurrent weight loss (Fig. 1c). By the end of the second week, the blood glucose levels in the STZ group exceeded 15 mM and remained elevated throughout the post-photothrombosis observation period, confirming the successful induction of chronic diabetes. The success of the photothrombotic stroke model was validated via laser speckle monitoring of cerebral blood flow, TTC staining, and Nissl staining (Fig. S1a–c). While control mice showed spontaneous functional recovery over time, DM significantly retarded this process. This impairment was evidenced by significantly worse performance in the foot fault (Fig. 1d) and Rotarod tests (Fig. 1e), as well as higher neurological deficit scores (Fig. 1f) compared to non-diabetic mice. These observations are consistent with previous reports suggesting that DM exacerbates neurovascular damage and obstructs brain repair, ultimately impairing post-stroke functional recovery (Zhang et al. 2016).

DM Reduces Functional Vascular Intensity and Angiogenesis in the Peri-Infarction Area Following Photothrombosis

Given the positive correlation between peri-infarct vascular intensity and stroke prognosis (Krupinski et al. 1994), we evaluated the functional blood vessels using tomato-lectin. As shown in Fig. 2a, compared with the corresponding position of the non-ischemic hemisphere in the control group, there was a significant decrease in the lectin-labeled functional blood vessels in the peri-infarction area of the ischemic hemisphere one day after focal ischemia. Vascular density in the peri-infarct area was significantly reduced in DM mice, whereas there was reparative neovascularization in the peri-infarction area of the ischemic hemisphere in control mice 7 days and 14 days after focal ischemia (Fig. 2a, b).

To determine if these changes were linked to active angiogenesis, we performed double immunofluorescent staining for CD31 and Ki67 in the brain slices. In control mice, prominent Ki67-positive signals were observed in peri-infarct blood vessels 7 days post-stroke; however, this angiogenic response was significantly diminished in the DM group (Fig. 2c, d).

DM Impairs BBB Integrity, Pericyte Coverage and White Matter Integrity After Photothrombosis

BBB integrity was assessed by measuring IgG leakage (Wang et al. 2016) via western blot and immunofluorescence. Our results showed that while there was no significant difference in IgG leakage between the DM and control group 1 day post-stroke (Fig. 3a), DM mice exhibited significantly higher leakage at 7 and 14 days after photothrombosis-induced cerebral ischemia (Fig. 3b), indicating exacerbated long-term BBB damage. Fluorescence results confirmed that the DM-induced IgG leakage increased after photothrombosis-induced cerebral ischemia (Fig. 3c). Moreover, pericyte coverage, a critical factor for BBB stabilization and recovery (Yang and

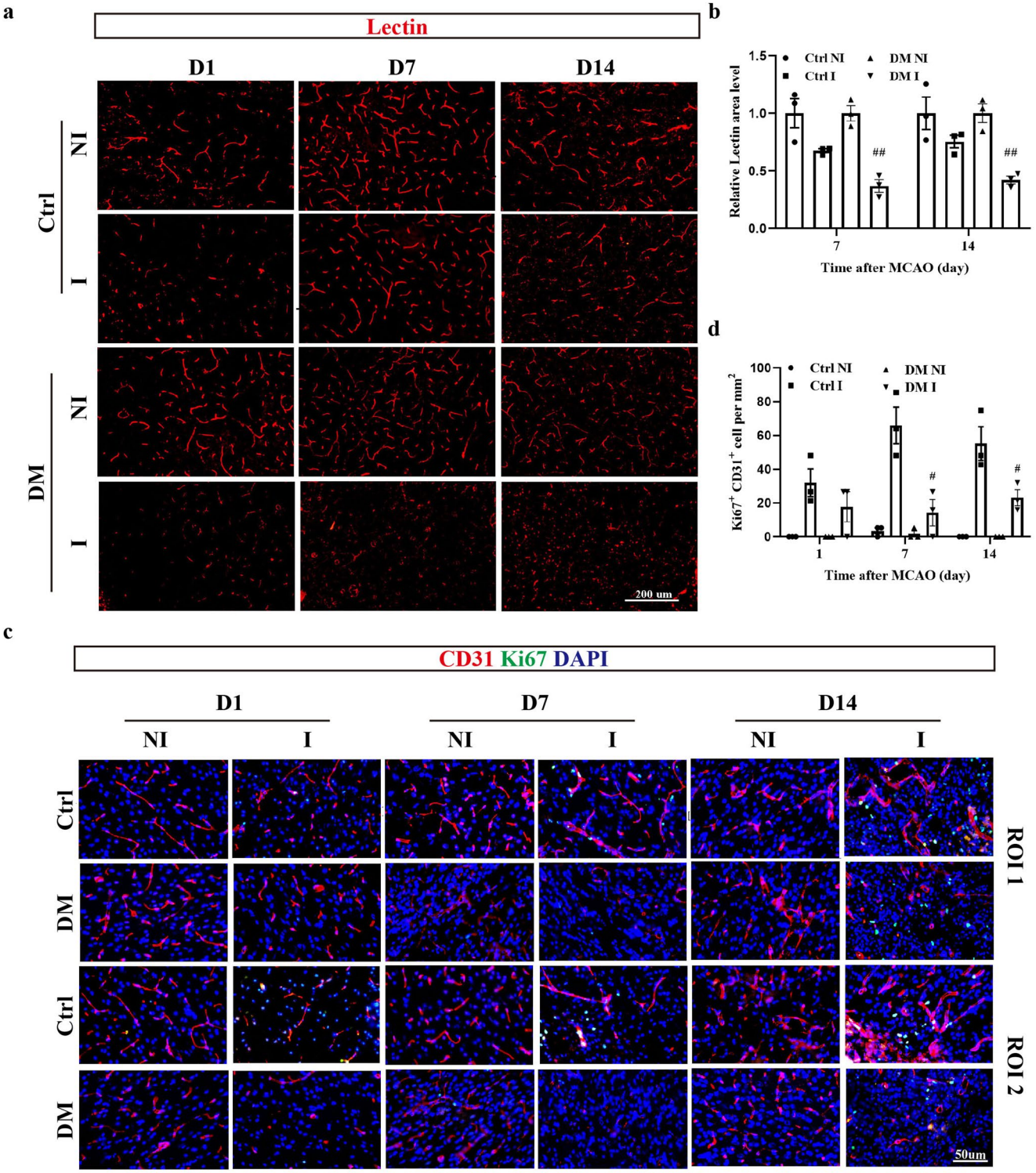

Fig. 2 DM significantly decreased the functional vascular density and angiogenesis in the peri-infarction area after photothrombosis. **a** Compared with the non-ischemic hemisphere, the functional vascular labeling of the ischemic hemisphere lectin is reduced 1 day after ischemia. As the ischemia duration is prolonged, the density of functional vascular labeling marked by lectin increases, and the length of blood vessels increases 14 days after ischemia. The functional blood vessel density in the peri-infarction area in the DM group is significantly reduced at 1 day, 7 days, and 14 days ($n = 3$/group, scale bar = 200 μm). **b** Quantification of lectin-positive vessels in the Ctrl and DM group 7 and 14 days after PT. **c** DM significantly decreased angiogenesis detected by Ki67 (green) and CD31 (red) double staining 7 and 14 days after ischemia. **d** Quantification of Ki67- and CD31-positive cells in Ctrl and DM group 1, 7 and 14 days after PT. (NI, Non-ischemic hemisphere; I, ischemic hemisphere. ROI: region of interest. $n = 3$/group, Scale bar = 50 μM)

https://doi.org/10.1007/s10571-026-01811-w

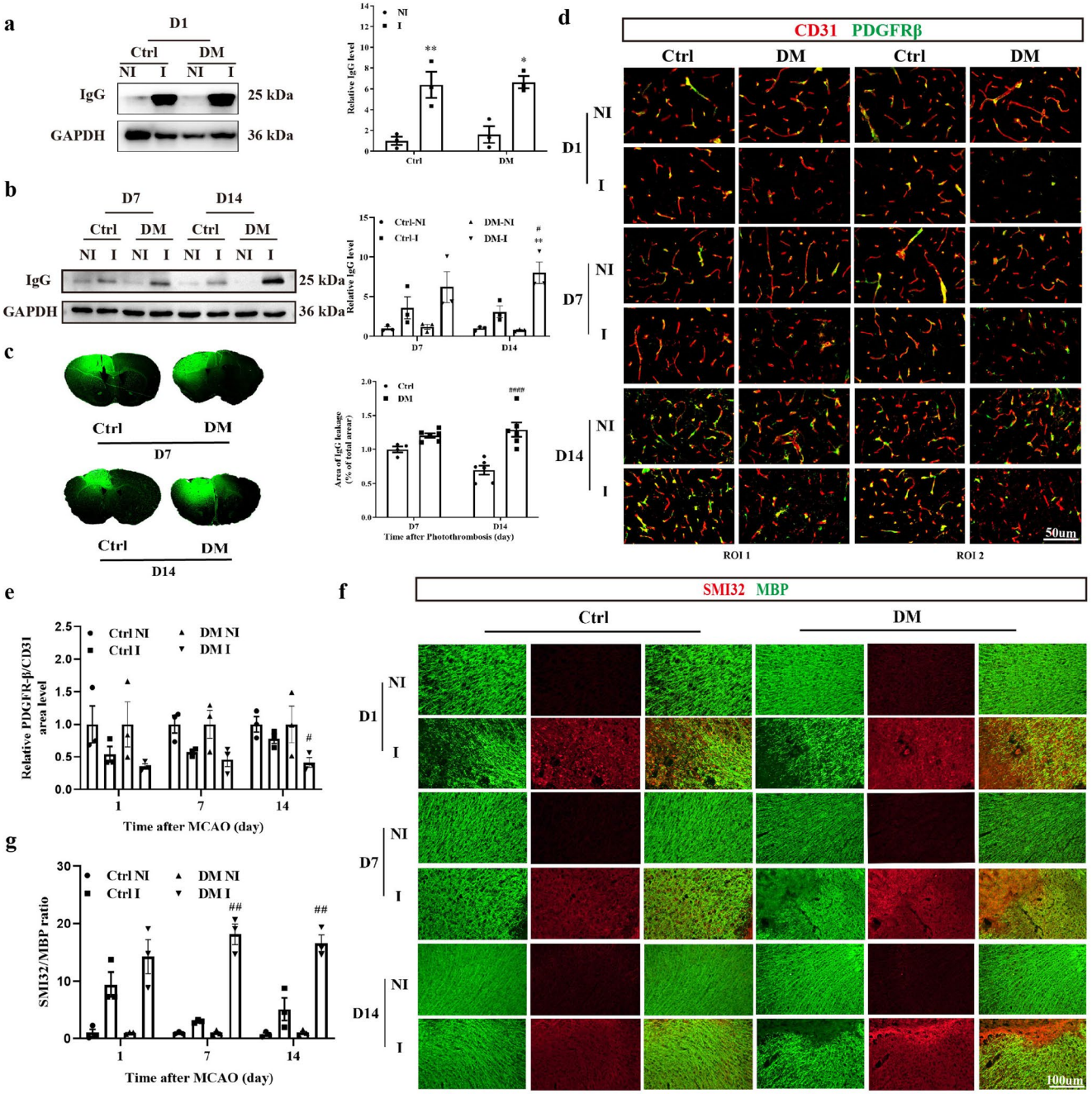

Fig. 3 DM impairs BBB integrity 7 and 14 days after photothrombosis. **a**, **b** Western blot results showed that significant IgG leakage was detected in the ischemic hemisphere, and DM significantly increased the IgG leakage 7 and 14 days after PT (b, $n=3$/group). **c** Seven and fourteen days after ischemia, immunofluorescence staining showed that there was significant IgG leakage in the ischemic hemisphere, and DM significantly increased the IgG leakage ($n=4$–6/group). **d** Compared to the non-ischemic hemisphere, pericyte coverage stained by PDGF-β was significantly increased 7 or 14 days after ischemia. DM decreases pericyte coverage. **e** The vessel that were covered by pericytes was quantitated; DM significantly decreased pericyte coverage after PT ($n=3$/group, Scale bar = 50 μm). **f** Ischemia induced significant MBP degradation, which was further exaggerated by DM after PT. **g** quantification of SIM32/MBP, DM significantly increased SIM32 and decreased MBP ($n=3$/group, Scale bar = 100 μm, $^{*}P<0.05$, $^{**}P<0.01$, vs. NI, $\#P<0.05$, $\#\#P<0.01$ vs. Ctrl. NI, non-ischemic hemisphere; I, ischemic hemisphere)

Torbey 2020), was significantly inhibited in DM mice, as shown by PDGFR-β and CD31 co-staining (Fig. 3d, e). Furthermore, DM exacerbated the ischemia-induced SMI32 increase and MBP degradation (Fig. 3f, g), suggesting that DM-mediated functional deficits are also linked to aggravated white matter injury.

DM Suppresses the Expression of Tight Junction Proteins After Photothrombosis

We examined the expression of Tight junction proteins claudin-5, occludin, and ZO-1, which play a critical role in maintaining BBB integrity (Wang et al. 2023d; Zhang et al. 2024). Double immunostaining of claudin-5 and CD31 showed that the expression levels of claudin-5 in the microvessels of the ischemic hemisphere were significantly reduced on day 1, and there was a recovery on day 7 and day 14. DM significantly hindered the recovery of claudin-5 in the microvessels of the ischemic hemisphere (Fig. 4a, upper panel). To more clearly visualize the common positioning of claudin-5 and CD31, high-magnification images of claudin-5 and CD31 co-staining were shown in Fig. 4a (lower panel). The expression levels of claudin-5 were not significantly recovered with the extension of the reperfusion duration, indicating that the DM inhibited claudin-5 expression.

Western blot results showed that compared to the non-ischemic hemisphere, while the expression levels of ZO-1, occludin, and claudin-5 in the ischemic hemisphere were initially dropped on day 1, they gradually recovered in control mice by day 7 and day 14. In contrast, DM significantly hindered the recovery of claudin-5 (Fig. 4b), occludin (Fig. 4c), and ZO1 (Fig. 4d, e) in the ischemic hemisphere.

DM Inhibits the Expression of Robo1, and Increases the Expression of Robo4, But Does Not Affect slit2 Expression After Photothrombosis

Robo1 is known to promote retinal angiogenesis in the mouse postnatal retina and in a model of ocular neovascular disease (Rama et al. 2015). Using immunofluorescence double staining, we first confirmed that Robo1 is expressed in microvessels. DM significantly inhibited the post-stroke Robo1 increase in the peri-infarction area of the ischemic hemisphere on day 7 (Fig. 5a) and day 14 (Fig. S2a). The results were further confirmed by western blot showing that DM significantly downregulated the post-stroke expression levels of Robo1 on day 1 (Fig. 5b), day 7, and day 14 (Fig. 5c), suggesting that DM may impair angiogenesis by inhibiting Robo1expression in a time-dependent manner.

Slit2-Robo4 signaling pathway was reported to play a role in inhibiting angiogenesis (Barquilla and Pasquale 2015; Hoang et al. 2009; Köhler et al. 2013). Robo4, another receptor of the factor Slit2, was related to angiogenesis after the stroke (Jones et al. 2008). Compared to the non-ischemic hemisphere, there was a significant decrease in Robo4 expression levels in microvessels in the peri-infarction area of the ischemic hemisphere, detected by immunofluorescence. DM significantly upregulated the expression levels of Robo4 on Day 7 (Fig. 5d). The results were further corroborated by western blot, showing that DM significantly upregulated the poststroke expression of Robo4 on Day 1 (Fig. 5e), Day 7, but not Day 14 (Fig. 5f). These results suggest that DM may impair angiogenesis by promoting the expression of Robo4 in a time-dependent manner.

Using immunofluorescence double staining, we confirmed that Slit2 was expressed in microvessels. Focal ischemia did not affect the expression of Slit2, and DM did not affect the protein expression of Slit2 on Day 7 (Fig. 5g) and Day 14 (Fig. S2c). Western blot results showed that there was no significant change in Slit2 expression levels on Day 1 (Fig. 5h), Day 7 (Fig. 5i), and Day 14 (Fig. S2f).

DM Inhibits the Expression of CRTC1 After Photothrombosis

The expression of CRTC1 has been shown to play a role in BBB damage after focal ischemia (Chen et al. 2022); it is not clear whether it plays a role in BBB repair. Using immunofluorescence double staining, our results confirmed that CRTC1 was expressed in microvessels. Ischemia induced significant CRTC1 degradation, which was further exacerbated by DM on day 7 (Fig. 6a) and day 14 (Fig. 6b). The results were further confirmed by western

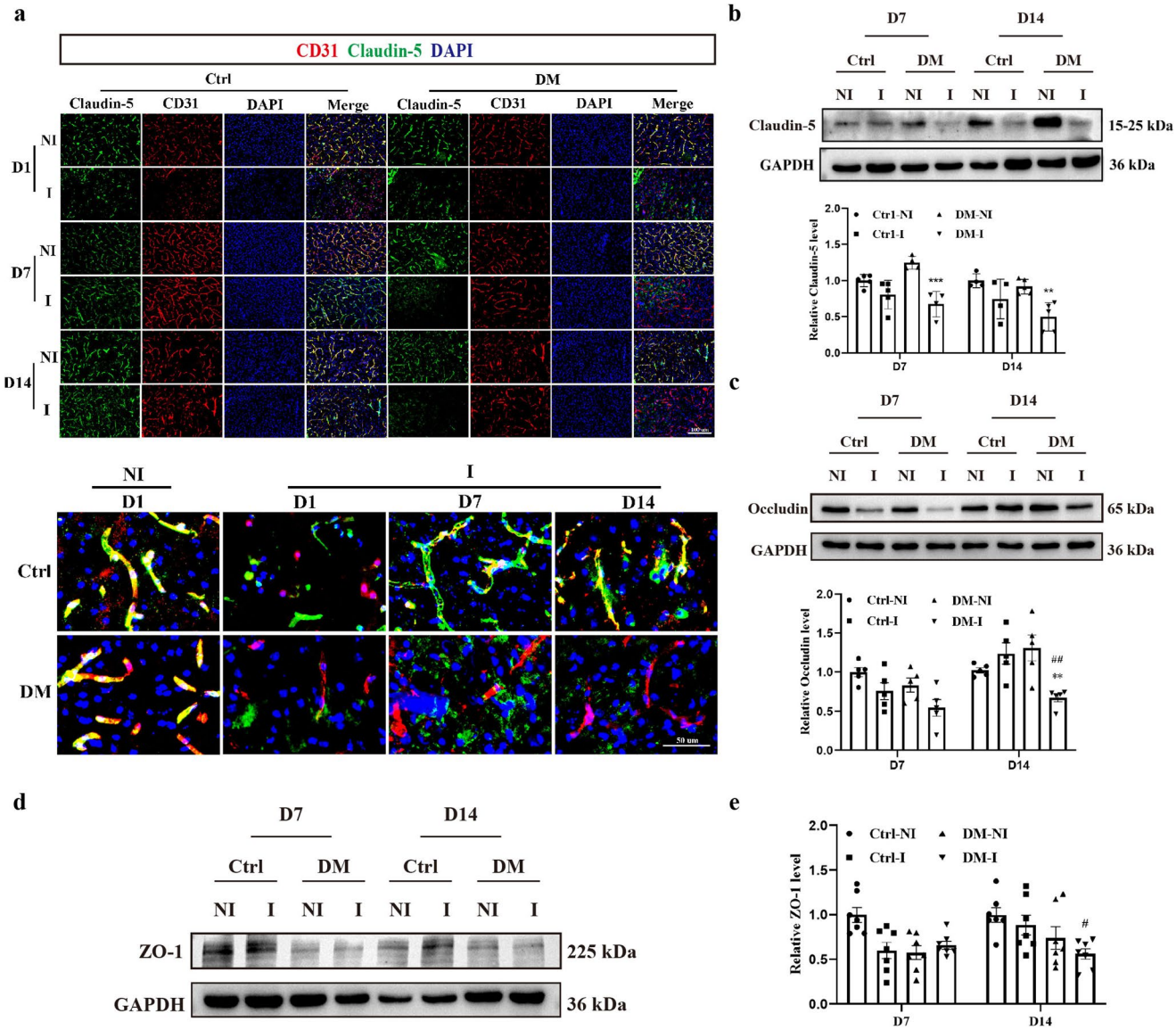

Fig. 4 DM decreases the expression of tight junction proteins 7 and 14 days after photothrombosis. **a** Representative immunofluorescence images of CD31 and claudin-5 staining in the Ctrl and DM groups at days 1, 7, and 14 post-PT (upper panel, $n=3$/group, scale bar = 100 μm). Representative higher-magnification immunofluorescence images showed that CD31 and claudin-5 co-staining in the Ctrl group at day 1 post-PT, and in the DM group at day 1, 7, and 14 post-PT (lower panel, $n=3$/group, scale bar = 50 μm). **b** Representative western blot images (upper panel) and quantitative analysis (lower panel) of claudin-5 in the Ctrl and DM groups at days 7 and 14 post-PT showed that DM significantly reduced claudin-5 expression after PT ($n=4$–5/group). Representative western blot images (upper panel) and quantitative analysis (lower panel) of occludin (**c**) and ZO-1 (**d**, **e**) in the Ctrl and DM groups at days 7 and 14 post-PT demonstrated that DM markedly decreased the expression of both occludin and ZO-1 after PT ($n=5$–7/group). NI nonischemic, I ischemic, *$p<0.05$, **$p<0.01$, ***$p<0.001$ vs. the NI, #$p<0.05$, ##$p<0.01$ vs. the Ctrl group

blot, showing that CRTC1 expression in the peri-infarction area of the ischemic hemisphere was significantly decreased relative to the non-ischemic hemisphere. Additionally, DM further decreased CRTC1 expression on day 1 (Fig. 6c), day 7, and day 14 (Fig. 6d), suggesting that suppressed CRTC1 expression may contribute to impaired BBB repair in diabetic conditions.

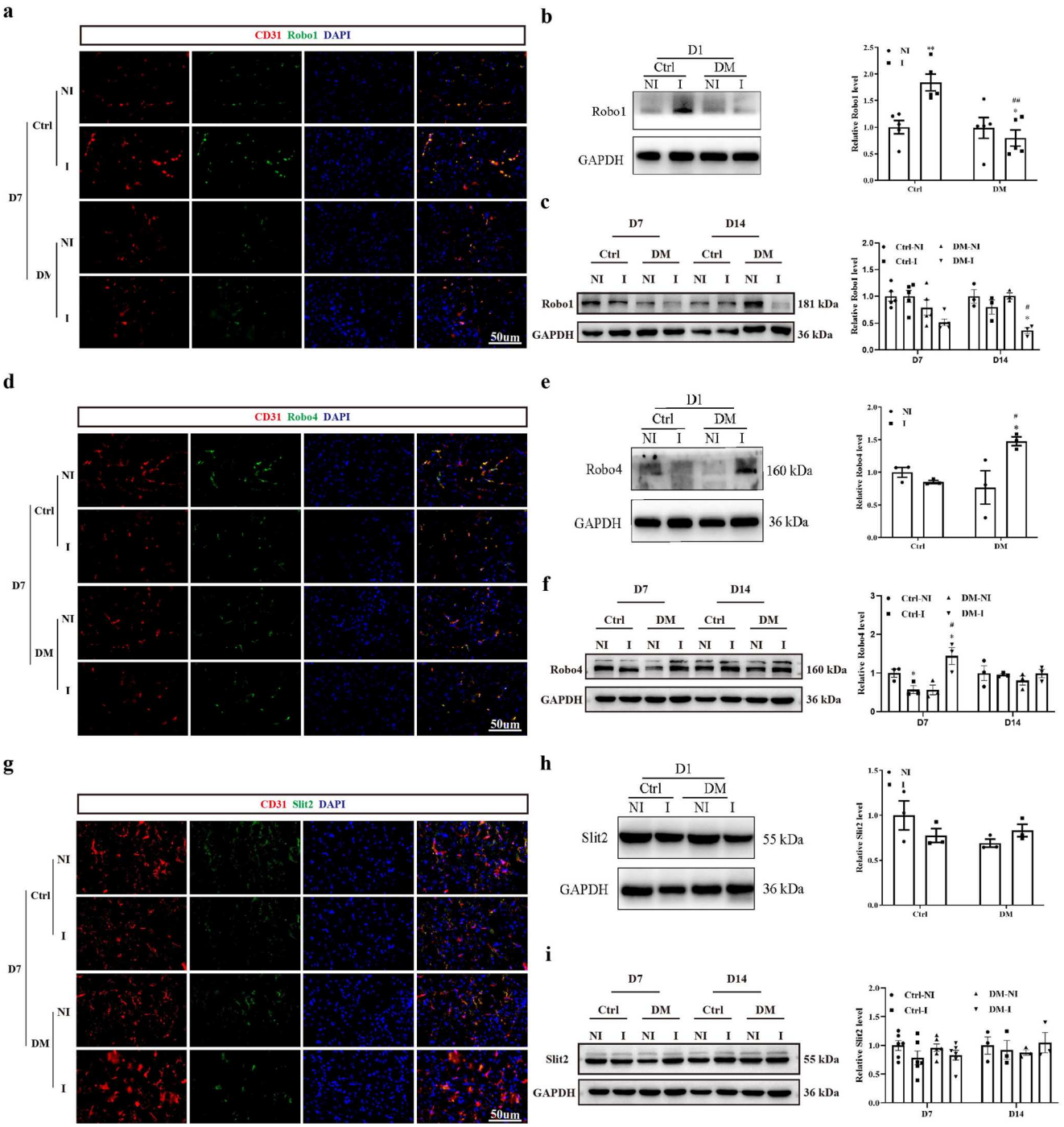

Fig. 5 DM decreased Robo1 expression, increased Robo4 expression, and did not alter Slit2 in the peri-infarction area after photothrombosis. **a** Representative images of CD31 and Robo1 immunofluorescence staining in the Ctrl and DM groups at day 7 post-PT ($n=3$/group, scale bar=50 μm). **b**, **c** Representative western blot image and quantitative analysis of Robo1 in the Ctrl and DM groups at day 1 (**b**), 7, and 14 (**c**) post-PT showed that DM markedly reduced Robo1 levels at 1, 7, and 14 days after PT ($n=3$–5/group). **d** The representative images of CD31 and Robo4 immunofluorescence staining in the Ctrl and DM groups at day 7 post-PT ($n=3$/group, scale bar = 50 μm). **e**, **f** Representative western blot image and quantitative analysis of Robo4 in the Ctrl and DM groups at day 1 (**e**), 7, and 14 (**f**) post-PT showed that DM significantly increased Robo4 levels 7 days after PT ($n=3$/group). **g** The representative images of CD31 and Slit2 immunofluorescence staining in the Ctrl and DM groups at day 7 post-PT ($n=3$/group, scale bar=50 μm). **h**, **i** Representative western blot image and quantitative analysis of Slit2 in the Ctrl and DM groups at day 1 (**h**) and 7 and 14 days (**i**) post-PT showed that there was no significant change in Slit2 level in the DM group after PT ($n=3$–6/group). NI, nonischemic; I, ischemic, $*p<0.05$, $**p<0.01$, $***p<0.001$ vs. the NI, $\#p<0.05$, $\#\#p<0.01$ vs. the Ctrl group

https://doi.org/10.1007/s10571-026-01811-w

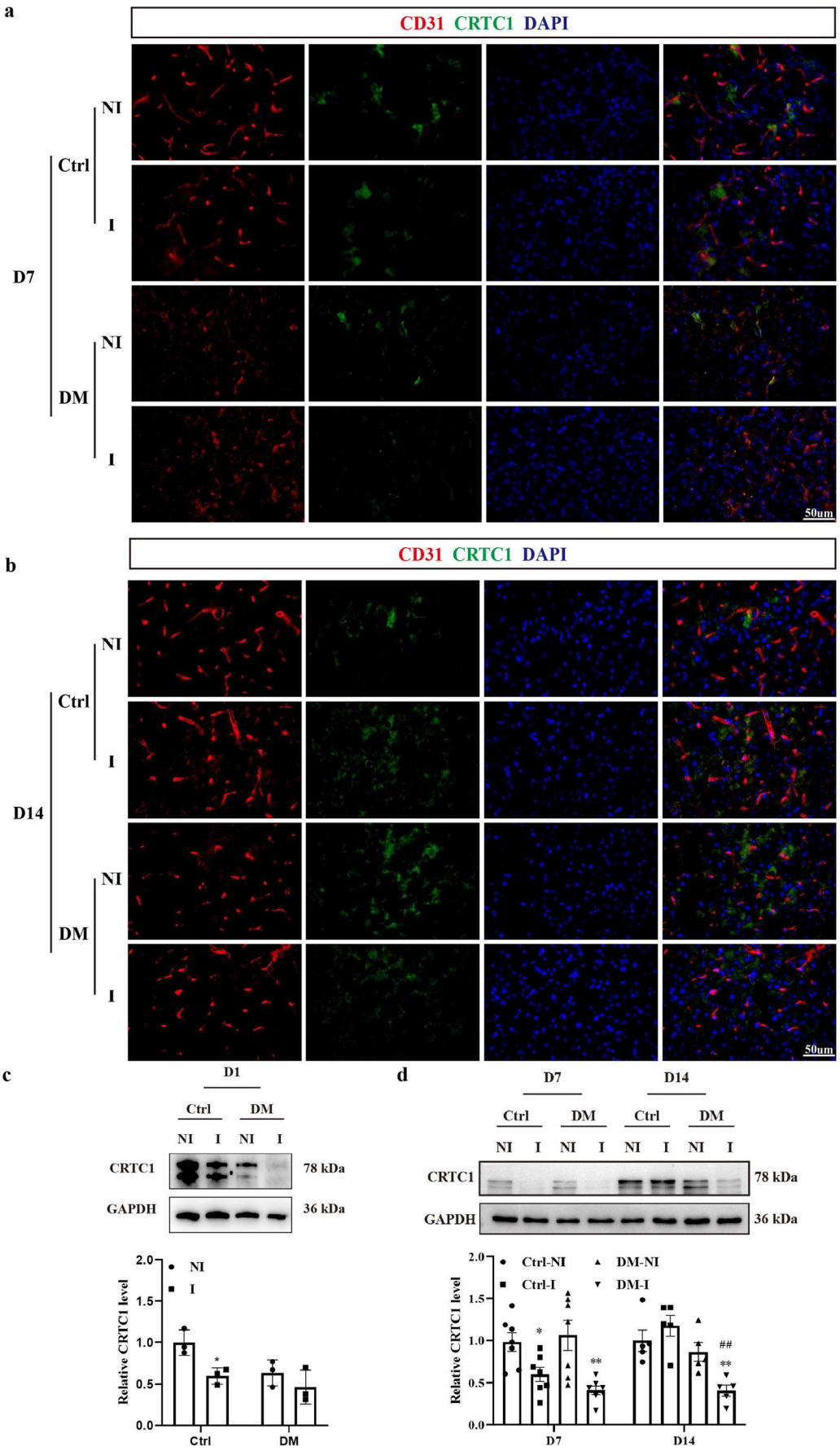

Fig. 6 DM decreased the expression of CRTC1 in the peri-infarction area after photothrombosis. **a**, **b** The representative images of CRTC1 and CD31 immunofluorescence staining in the Ctrl and DM groups at days 7 (**a**) and 14 (**b**) post-PT ($n=3$/group, scale bar = 50 μm). **c** Representative western blot image and quantitative analysis of CRTC1 in the Ctrl and DM groups at days 1 (**c**), 7, and 14 (**e**) post-PT showed that the level of CRTC1 in the DM group was markedly decreased at day 14 after PT ($n=3$–7/group). NI nonischemic, I ischemic. *$p<0.05$, **$p<0.01$, ***$p<0.001$ vs. the NI, ##$p<0.01$, vs.

Discussion

DM significantly exacerbates motor and cognitive deficits following stroke (Kuwashiro et al. 2013). Because angiogenesis and the maintenance of BBB integrity are fundamental to functional recovery after ischemic stroke (Yang and Torbey 2020), understanding how DM impairs these processes is vital. In the present study, using the mouse photothrombosis model, we investigated the impact of DM on post-stroke angiogenesis and BBB integrity and the Slit2/Robo/CRTC1 signaling pathway after photothrombosis. Our primary findings indicate that: (1) DM impairs neurological recovery and reduces both functional vessel density and active angiogenesis in the ischemic penumbra; (2) DM disrupts BBB integrity by decreasing tight junction protein expression and pericyte coverage at 7 and 14 days post-stroke; (3) DM leads to a significant decrease in Robo1 and an increase in Robo4 expression without altering Slit2 levels; (4) DM suppresses the expression of CRTC1 in the ischemic penumbra.

Previous studies have shown that while spontaneous brain repair occurs following acute stroke (Li et al. 2020), DM can worsen the motor and cognitive recovery after stroke. For example, Type 1 DM impairs cognitive function in middle-aged rats and neurological recovery in middle-aged rats after stroke (Zhang et al. 2016). In the present study, using mice photothrombosis model, we demonstrated that DM impairs motor function, as evidenced by Rotarod and foot-fault tests, and results in poor sensorimotor outcomes as measured by neurological scores. Since white matter integrity and angiogenesis are essential for functional recovery (Du et al. 2026b), we examined these pathways and found that DM significantly decreased MBP expression while increasing SMI-32 (a marker of axonal damage). These findings suggest that DM-induced functional decline is closely linked to structural white matter injury and impaired angiogenic processes.

Poststroke angiogenesis is essential for restoring oxygen and nutrient supply to injured tissues, providing neurotrophic support for concurrent neurogenesis and synaptogenesis, which ultimately lead to functional recovery (Xu et al. 2025). Clinical evidence have shown that vascular density in the penumbra after cerebral ischemia correlates positively with stroke patient prognosis and long-term survival (Krupinski et al. 1994). Moreover, pathologic analysis and brain imaging studies of patients with subacute and chronic stroke have found that the level of angiogenesis and vascular network reconstruction in the ischemic penumbra determines the long-term survival rate of patients (Liu et al. 2014). While DM is known to cause pathological neovascularization in the retina, it paradoxically impairs restorative angiogenesis in the heart and peripheral limbs, it paradoxically impairs restorative angiogenesis in the heart and peripheral limbs (Ergul et al. 2014). In the present study, our results align with findings in Type 2 diabetic models where impaired collateral flow contributes to poor stroke outcomes (Akamatsu et al. 2015). Here, we demonstrate that DM reduces functional blood vessel density, suggesting that suppressed angiogenesis is a primary driver of DM-induced recovery failure.

For neovascularization to be truly "functional," vessels must mature through the expression of tight junction proteins and recruitment of pericytes (Bai et al. 2026). Without these elements, new vessels remain "leaky" or non-perfused. This explains why some studies observe increased microvascular density without a corresponding increase in cerebral blood flow (Wang et al. 2012), or find "empty" microvessels that fail to provide perfusion (Yu et al. 2007). In the present study, our results show that DM decreases tight junction proteins and pericyte coverage, leading to compromised BBB integrity. These findings reinforce the idea that protecting the BBB is as critical as promoting vessel growth for improving motor and cognitive outcomes (Liu et al. 2017). Current strategies to promote angiogenesis often rely on VEGF; however, VEGF-induced vessels are frequently immature, leading to increased BBB leakage (Rust et al. 2019a, 2019b) and brain edema (Reischl et al. 2014). Consequently, identifying alternative pathways such as axon guidance molecules, including Netrins, Ephrins, and Semaphorin 3, is a priority. The Slit2 signaling pathway is a promising candidate, as its effect on endothelial cells depends on the balance between Robo1 and Robo4 receptors (Rust et al. 2019b). Consistent with a previous study showing that Slit2/Robo1 signaling is involved in angiogenesis of glomerular endothelial cells exposed to a diabetic-like environment (Liu et al. 2018), our results indicate that DM shifts this balance by decreasing Robo1 and upregulating Robo4. This supports previous models suggesting that Slit2-Robo1 signaling stimulates angiogenesis, while

Slit2-Robo4 signaling inhibits it (Barquilla and Pasquale 2015; Hoang et al. 2009; Köhler et al. 2013), suggesting that there is functional divergence between Robo1 and Robo4, particularly in the context of post-stroke vascular remodeling and BBB integrity, and that differential regulation under diabetic conditions has significant biological implications.

Endothelial cell-specific CRTC2-knock-out mice showed reduced angiogenesis, exacerbated stroke, and impaired neurologic recovery (Kanki et al. 2020). In the present study, we observed a significant reduction in CRTC1 expression in diabetic mice. As CRTC1 expression mirrored that of Robo1, we hypothesize that (1) CRTC1 serves as a downstream target of the Slit2-Robo pathway. In its dephosphorylated state, CRTC1 translocates from the cytosol to the nucleus to act as a transcriptional co-activator; (2) Slit2-Robo signaling pathway regulates angiogenesis and BBB repair by regulating the phosphorylated and non-phosphorylated forms of CRTC1 and neurological recovery (Wang et al. 2023b). Therefore, based on our results, it is plausible that DM may disrupt the phosphorylation state of CRTC1 via the Slit2-Robo pathway, thereby suppressing the transcriptional programs necessary for angiogenesis and BBB repair.

While this study elucidates how DM impairs post-stroke angiogenesis and BBB integrity, several limitations regarding clinical translation remain. Only male animals are used; only photothrombosis is used; there are no rescue experiments.

In summary, we demonstrate that DM-induced functional deficits after stroke are closely tied to the impairment of angiogenesis and BBB integrity. The downregulation of Robo1 and CRTC1, coupled with the upregulation of Robo4, provides a mechanistic explanation for this vascular failure. Our findings suggest that the Slit2/Robo1/CRTC1 axis is a viable therapeutic target for promoting vascular repair and functional recovery in diabetic stroke patients.

Supplementary Information The online version contains supplementary material available at https://doi.org/10.1007/s10571-026-01811-w.

Acknowledgements This work was supported by the Medical and Health Science and Technology Plan Project of Zhejiang Province (2024KY1685), Zhejiang Provincial Natural Science Foundation of China (LTGY24H090002), and Jiaxing Plan of Science and Technology (2025CGZ064).

Author Contributions YPW gets the funding. YH, XS, XZ, XL, JG, HG, YHW, XW, CX, MS, YS, participated in the study design, performed the experiments, and made the figures. YH, YPW, and SQ interpreted the data and drafted the manuscript. CG revised the manuscript. YPW and XJ supervised the study, reviewed the original data, and finalized the manuscript. All authors have read and approved the final manuscript.

Data Availability The data are available upon reasonable request.

Declarations

Competing Interests The authors declare no competing interests.

Ethical Approval and Consent to Participate All animal experiments are conduct following ethical policies and procedures approved by the Capital Medical University ethics committee (Ethical inspection No. AEEI-2023-014).

References

Abdelsaid M, Prakash R, Li W, Coucha M, Hafez S, Johnson MH, Fagan SC, Ergul A (2015) Metformin treatment in the period after stroke prevents nitrative stress and restores angiogenic signaling in the brain in diabetes. Diabetes 64:1804–1817

Adams RH, Eichmann A (2010) Axon guidance molecules in vascular patterning. Cold Spring Harb Perspect Biol 2:a001875

Akamatsu Y, Nishijima Y, Lee CC, Yang SY, Shi L, An L, Wang RK, Tominaga T, Liu J (2015) Impaired leptomeningeal collateral flow contributes to the poor outcome following experimental stroke in the Type 2 diabetic mice. J Neurosci 35:3851–3864

Bai J, Yang J, Liu W, Han B, Jiang S, Sun J, Qi H (2026) Extracellular vesicles: Revolutionizing targeted therapy for ischemic stroke. Acta Pharm Sin B 16:2838–2876

Barquilla A, Pasquale EB (2015) Eph receptors and ephrins: therapeutic opportunities. Annu Rev Pharmacol Toxicol 55:465–487

Beck H, Plate KH (2009) Angiogenesis after cerebral ischemia. Acta Neuropathol 117:481–496

Chen R, Zhang MQ, Miao YL, Zhang SH, Cheng Y, Wang SS, Yin J, Yang CH, Zhang HF, Tang L, Li Y, Zhang Y, Fan YY (2024) Targeting neuronal GPR65 with delayed BTB09089 treatment improves neurorehabilitation following ischemic stroke. Stroke 55:2151–2162

Chen S, Sun Y, Li F, Zhang X, Hu X, Zhao X, Li Y, Li H, Zhang J, Liu W, Zheng GQ, Jin X (2022) Modulation of alpha7nAchR by melatonin alleviates ischemia and reperfusion-compromised integrity of blood-brain barrier through inhibiting hmgb1-mediated microglia activation and crtc1-mediated neuronal loss. Cell Mol Neurobiol 42:2407–2422

Coll M, Arino S, Martinez-Sanchez C, Garcia-Pras E, Gallego J, Moles A, Aguilar-Bravo B, Blaya D, Vallverdu J, Rubio-Tomas T, Lozano JJ, Pose E, Graupera I, Fernandez-Vidal A, Pol A, Bataller R, Geng JG, Gines P, Fernandez M, Sancho-Bru P (2022) Ductular reaction promotes intrahepatic angiogenesis through Slit2-Roundabout 1 signaling. Hepatology 75:353–368

Du W, Geng P, Lian Z, Sun Y, Zhou Y, Guo C, Jin X (2026a) DPSCs-Exos promote OPCs differentiation and white matter repair via Myl9-mediated PRMT5 nucleation after ischemic stroke. J Cereb Blood Flow Metab 46:695–709

Du W, Liu W, Sun Y, Guo C, Geng P, Jin X (2026b) Targeting angiogenesis and white matter repair for enhanced functional recovery after acute ischemic stroke: A focus on the roles of glial cells. J Cereb Blood Flow Metab 46:3–19

Du WH, Guo H, Wang YH, Hu XY, Zhang JN, Guo C, Geng PP, Wang YJ, Jin XC (2026c) TNF-alpha/PAD4 axis drives hyperhomocysteine-induced white matter injury after acute ischemic stroke. Acta Pharmacol Sin 47:2035–2048

Ergul A, Abdelsaid M, Fouda AY, Fagan SC (2014) Cerebral neovascularization in diabetes: implications for stroke recovery and beyond. J Cereb Blood Flow Metab 34:553–563

Guo W, Hu C, Wang Y, Zhang W, Zhang S, Peng J, Wang Y, Wu J (2025) NO-releasing double-crosslinked responsive hydrogels accelerate the treatment and repair of ischemic stroke. Acta Pharm Sin B 15:1112–1125

Hoang S, Liauw J, Choi M, Choi M, Guzman RG, Steinberg GK (2009) Netrin-4 enhances angiogenesis and neurologic outcome after cerebral ischemia. J Cereb Blood Flow Metab 29:385–397

Hu X, Dong J, Geng P, Sun Y, Du W, Zhao X, Wang Q, Liu C, Wang X, Liu Y, Liu W, Cheng H, Wang W, Jin X (2024) Nicotine treatment ameliorates blood-brain barrier damage after acute ischemic stroke by regulating endothelial scaffolding protein Pdlim5. Transl Stroke Res 15:672–687

Jones CA, London NR, Chen H, Park KW, Sauvaget D, Stockton RA, Wythe JD, Suh W, Larrieu-Lahargue F, Mukouyama YS, Lindblom P, Seth P, Frias A, Nishiya N, Ginsberg MH, Gerhardt H, Zhang K, Li DY (2008) Robo4 stabilizes the vascular network by inhibiting pathologic angiogenesis and endothelial hyperpermeability. Nat Med 14:448–453

Kanki H, Sasaki T, Matsumura S, Kawano T, Todo K, Okazaki S, Nishiyama K, Takemori H, Mochizuki H (2020) CREB coactivator CRTC2 plays a crucial role in endothelial function. J Neurosci 40:9533–9546

Köhler D, Streißenberger A, König K, Granja T, Roth JM, Lehmann R, de Oliveira Franz CB, Rosenberger P (2013) The uncoordinated-5 homolog B (UNC5B) receptor increases myocardial ischemia-reperfusion injury. PLoS One 8:e69477

Krupinski J, Kaluza J, Kumar P, Kumar S, Wang JM (1994) Role of angiogenesis in patients with cerebral ischemic stroke. Stroke 25:1794–1798

Kuwashiro T, Sugimori H, Ago T, Kuroda J, Kamouchi M, Kitazono T (2013) The impact of predisposing factors on long-term outcome after stroke in diabetic patients: the Fukuoka Stroke Registry. Eur J Neurol 20:921–927

Li F, Liu WC, Wang Q, Sun Y, Wang H, Jin X (2020) NG2-glia cell proliferation and differentiation by glial growth factor 2 (GGF2), a strategy to promote functional recovery after ischemic stroke. Biochem Pharmacol 171:113720

Liu J, Hou W, Guan T, Tang L, Zhu X, Li Y, Hou S, Zhang J, Chen H, Huang Y (2018) Slit2/Robo1 signaling is involved in angiogenesis of glomerular endothelial cells exposed to a diabetic-like environment. Angiogenesis 21:237–249

Liu J, Wang Y, Akamatsu Y, Lee CC, Stetler RA, Lawton MT, Yang GY (2014) Vascular remodeling after ischemic stroke: mechanisms and therapeutic potentials. Prog Neurobiol 115:138–156

Liu Y, Liu WC, Sun Y, Shen X, Wang X, Shu H, Pan R, Liu CF, Liu W, Liu KJ, Jin X (2017) Normobaric hyperoxia extends neuro- and vaso-Protection of N-acetylcysteine in transient focal ischemia. Mol Neurobiol 54:3418–3427

Martini SR, Kent TA (2007) Hyperglycemia in acute ischemic stroke: a vascular perspective. J Cereb Blood Flow Metab 27:435–451
McCormick MT, Muir KW, Gray CS, Walters MR (2008) Management of hyperglycemia in acute stroke: how, when, and for whom? Stroke 39:2177–2185
Peng C, Yang LJ, Zhang C, Jiang Y, Shang LW, He JB, Zhou ZW, Tao X, Tie L, Chen AF, Xie HH (2023) Low-dose nifedipine rescues impaired endothelial progenitor cell-mediated angiogenesis in diabetic mice. Acta Pharmacol Sin 44:44–57
Prakash R, Li W, Qu Z, Johnson MA, Fagan SC, Ergul A (2013) Vascularization pattern after ischemic stroke is different in control versus diabetic rats: relevance to stroke recovery. Stroke 44:2875–2882
Qi Z, Liang J, Pan R, Dong W, Shen J, Yang Y, Zhao Y, Shi W, Luo Y, Ji X, Liu KJ (2016) Zinc contributes to acute cerebral ischemia-induced blood-brain barrier disruption. Neurobiol Dis 95:12–21
Rama N, Dubrac A, Mathivet T, Ni Charthaigh RA, Genet G, Cristofaro B, Pibouin-Fragner L, Ma L, Eichmann A, Chedotal A (2015) Slit2 signaling through Robo1 and Robo2 is required for retinal neovascularization. Nat Med 21:483–491
Reischl S, Li L, Walkinshaw G, Flippin LA, Marti HH, Kunze R (2014) Inhibition of HIF prolyl-4-hydroxylases by FG-4497 reduces brain tissue injury and edema formation during ischemic stroke. PLoS One 9:e84767
Romano E, Manetti M, Rosa I, Fioretto BS, Ibba-Manneschi L, Matucci-Cerinic M, Guiducci S (2018) Slit2/Robo4 axis may contribute to endothelial cell dysfunction and angiogenesis disturbance in systemic sclerosis. Ann Rheum Dis 77:1665–1674
Rust R, Gantner C, Schwab ME (2019a) Pro- and antiangiogenic therapies: current status and clinical implications. FASEB J 33:34–48
Rust R, Gronnert L, Weber RZ, Mulders G, Schwab ME (2019b) Refueling the ischemic CNS: guidance molecules for vascular repair. Trends Neurosci 42:644–656
Sherchan P, Huang L, Akyol O, Reis C, Tang J, Zhang JH (2017) Recombinant Slit2 reduces surgical brain injury induced blood brain barrier disruption via Robo4 dependent Rac1 activation in a rodent model. Sci Rep 7:746
Shi Y, Fan S, Wang D, Huyan T, Chen J, Chen J, Su J, Li X, Wang Z, Xie S, Yun C, Li X, Tie L (2018) FOXO1 inhibition potentiates endothelial angiogenic functions in diabetes via suppression of ROCK1/Drp1-mediated mitochondrial fission. Biochim Biophys Acta Mol Basis Dis 1864:2481–2494
Suchting S, Heal P, Tahtis K, Stewart LM, Bicknell R (2005) Soluble Robo4 receptor inhibits in vivo angiogenesis and endothelial cell migration. FASEB J 19:121–123
Wang Q, Wang MW, Sun YY, Hu XY, Geng PP, Shu H, Wang XN, Wang H, Zhang JF, Cheng HQ, Wang W, Jin XC (2023a) Nicotine pretreatment alleviates MK-801-induced behavioral and cognitive deficits in mice by regulating Pdlim5/CRTC1 in the PFC. Acta Pharmacol Sin 44:780–790
Wang X, Liu Y, Sun Y, Liu W, Jin X (2016) Blood brain barrier breakdown was found in non-infarcted area after 2-h MCAO. J Neurol Sci 363:63–68
Wang Y, Du W, Sun Y, Zhang J, Ma C, Jin X (2023b) CRTC1 is a potential target to delay aging-induced cognitive deficit by protecting the integrity of the blood-brain barrier via inhibiting inflammation. J Cereb Blood Flow Metab 43:1042–1059
Wang Y, Liu W, Geng P, Du W, Guo C, Wang Q, Zheng GQ, Jin X (2023c) Role of crosstalk between glial cells and immune cells in blood-brain barrier damage and protection after acute ischemic stroke. Aging Dis 15:2507–2525
Wang Y, Wang X, Zhang X, Chen S, Sun Y, Liu W, Jin X, Zheng G (2020) D1 receptor-mediated endogenous tPA upregulation contributes to blood-brain barrier injury after acute ischaemic stroke. J Cell Mol Med 24:9255–9266
Wang YP, Du WH, Hu XY, Yu X, Guo C, Jin XC, Wang W (2023d) Targeting the blood-brain barrier to delay aging-accompanied neurological diseases by modulating gut microbiota, circadian rhythms, and their interplays. Acta Pharm Sin B 13:4667–4687
Wang Z, Tsai LK, Munasinghe J, Leng Y, Fessler EB, Chibane F, Leeds P, Chuang DM (2012) Chronic valproate treatment enhances postischemic angiogenesis and promotes functional recovery in a rat model of ischemic stroke. Stroke 43:2430–2436
Wicha P, Das S, Mahakkanukrauh P (2021) Blood-brain barrier dysfunction in ischemic stroke and diabetes: the underlying link, mechanisms and future possible therapeutic targets. Anat Cell Biol 54:165–177
Wong D, Tran M, Martinez J, Avila I, Arrieta A, Kalindjian K, Rathbun E, Vondriska TM, Small EM, Quijada P (2026) Slit2-robo signaling regulates angiogenesis and repair following myocardial infarction. J Mol Cell Cardiol 210:28–42
Xu A, Zhang H, Zhang Y, Wu J, Huang Z (2025) Ischemic stroke and intervention strategies based on the timeline of stroke progression: Review and prospects. Acta Pharm Sin B 15:4543–4581
Yan H, Kanki H, Matsumura S, Kawano T, Nishiyama K, Sugiyama S, Takemori H, Mochizuki H, Sasaki T (2021) MiRNA-132/212 regulates tight junction stabilization in blood-brain barrier after stroke. Cell Death Discov 7:380
Yang Y, Torbey MT (2020) Angiogenesis and blood-brain barrier permeability in vascular remodeling after stroke. Curr Neuropharmacol 18:1250–1265
Yu SW, Friedman B, Cheng Q, Lyden PD (2007) Stroke-evoked angiogenesis results in a transient population of microvessels. J Cereb Blood Flow Metab 27:755–763
Zhang L, Chopp M, Zhang Y, Xiong Y, Li C, Sadry N, Rhaleb I, Lu M, Zhang ZG (2016) Diabetes mellitus impairs cognitive function in middle-aged rats and neurological recovery in middle-aged rats after stroke. Stroke 47:2112–2118

Zhang X, Shen X, Dong J, Liu WC, Song M, Sun Y, Shu H, Towse CL, Liu W, Liu CF, Jin X (2019) Inhibition of reactive astrocytes with fluorocitrate ameliorates learning and memory impairment through upregulating CRTC1 and synaptophysin in ischemic stroke rats. Cell Mol Neurobiol 39:1151–1163

Zhang XL, Du WH, Qian SX, Lu XD, Yu X, Fang HL, Dong JL, Song M, Sun YY, Wu XQ, Shen YF, Hao YN, Shen MH, Zhou BQ, Wang YP, Xu CY, Jin XC (2024) Glial growth factor 2 treatment alleviates ischemia and reperfusion-damaged integrity of the blood-brain barrier through decreasing Mfsd2a/caveolin-1-mediated transcellular and Pdlim5/YAP/TAZ-mediated paracellular permeability. Acta Pharmacol Sin 45:2241–2252

Authors and Affiliations

Yanping Wang[1] · Xuemei Shi[2,3] · Xiaoyun Zhao[4] · Xudong Lu[1] · Jingxia Gu[1] · Hui Guo[4] · Yihui Wang[4] · Xiaoqiang Wu[1] · Congying Xu[1] · Minghui Shen[1] · Yufei Shen[1] · Chun Guo[5] · Yanan Hao[1] · Shuxia Qian[1] · Xinchun Jin[4]

✉ Yanan Hao
haoyanan51899@163.com

✉ Xinchun Jin
xinchunjin@gmail.com

[1] Department of Neurology, The Second Affiliated Hospital of Jiaxing University, Jiaxing, China

[2] JiaXing Key Laboratory of Fundamental and Clinical Research on Cerebral Protection in Acute Ischemic Cerebrovascular Disease (A), Jiaxing, China

[3] Department of Neurology, Zhejiang University of Traditional Chinese Medicine, Hangzhou, China

[4] Department of Histology and Embryology, School of Basic Medical Sciences, Advanced Innovation Center for Human Brain Protection, Capital Medical University, Beijing 100069, People's Republic of China

[5] School of Biosciences, University of Sheffield, Firth Court, Western Bank, Sheffield, UK